

This discussion paper is/has been under review for the journal Atmospheric Chemistry and Physics (ACP). Please refer to the corresponding final paper in ACP if available.

# Ozone variability and halogen oxidation within the Arctic and sub-Arctic springtime boundary layer

**J. B. Gilman<sup>1,2</sup>, J. F. Burkhardt<sup>3</sup>, B. M. Lerner<sup>1,2</sup>, E. J. Williams<sup>1,2</sup>, W. C. Kuster<sup>1</sup>, P. D. Goldan<sup>1,2</sup>, P. C. Murphy<sup>1,2</sup>, C. Warneke<sup>1,2</sup>, C. Fowler<sup>4</sup>, S. A. Montzka<sup>1</sup>, B. R. Miller<sup>1,2</sup>, L. Miller<sup>1,2</sup>, S. J. Oltmans<sup>1</sup>, T. B. Ryerson<sup>1</sup>, O. R. Cooper<sup>1,2</sup>, A. Stohl<sup>3</sup>, and J. A. de Gouw<sup>1,2</sup>**

<sup>1</sup>Earth System Research Laboratory (ESRL), NOAA, Boulder, CO, USA

<sup>2</sup>Cooperative Institute for Research in the Environmental Sciences (CIRES), Univ. of Colorado, Boulder, CO, USA

<sup>3</sup>Norwegian Institute for Air Research (NILU), Kjeller, Norway

<sup>4</sup>Colorado Center for Astrodynamic Research (CCAR), Univ. of Colorado, Boulder, CO, USA

Received: 6 May 2010 – Accepted: 9 June 2010 – Published: 29 June 2010

Correspondence to: J. B. Gilman (jessica.gilman@noaa.gov)

Published by Copernicus Publications on behalf of the European Geosciences Union.

ACPD

10, 15885–15919, 2010

## Ozone variability and halogen oxidation

J. B. Gilman et al.

Title Page

Abstract

Introduction

Conclusions

References

Tables

Figures

◀

▶

◀

▶

Back

Close

Full Screen / Esc

Printer-friendly Version

Interactive Discussion



## Abstract

The influence of halogen oxidation on the variabilities of ozone ( $O_3$ ) and volatile organic compounds (VOCs) within the Arctic and sub-Arctic atmospheric boundary layer was investigated using field measurements from multiple campaigns conducted in March and April 2008 as part of the POLARCAT project. For the ship-based measurements, a high degree of correlation ( $r=0.98$  for 544 data points collected north of  $68^\circ$  N) was observed between the acetylene to benzene ratio, used as a marker for halogen oxidation, and  $O_3$  signifying the vast influence of bromine oxidation throughout the ice-free regions of the North Atlantic. Concurrent airborne and ground-based measurements in the Alaskan Arctic substantiated this correlation and were used to demonstrate that halogen oxidation influenced  $O_3$  variability throughout the Arctic boundary layer during these springtime studies. Measurements aboard the R/V “Knorr” in the North Atlantic and Arctic Oceans provided a unique view of the transport of  $O_3$ -poor air masses from the Arctic Basin to latitudes as far south as  $52^\circ$  N. FLEXPART, a Lagrangian transport model, was used to quantitatively determine the exposure of air masses encountered by the ship to first-year ice (FYI), multi-year ice (MYI), and total ICE (FYI+MYI).  $O_3$  anti-correlated with the modeled total ICE tracer ( $r=-0.86$ ) indicating that up to 73% of the  $O_3$  variability measured in the Arctic marine boundary layer could be related to sea ice exposure.

## 1 Introduction

Long-term measurements of surface ozone ( $O_3$ ) in the Arctic have shown that the greatest interannual variability occurs in the late winter and spring (Oltmans and Komhyr, 1986). During the Arctic springtime, surface  $O_3$  can fluctuate between background levels of approximately 40 ppbv to near zero. While ozone depletion events (ODEs) are episodic in nature, they have been shown to occur perennially in the Arctic springtime boundary layer across the whole of the Arctic Basin (Oltmans and Komhyr,

## Ozone variability and halogen oxidation

J. B. Gilman et al.

Title Page

Abstract

Introduction

Conclusions

References

Tables

Figures

◀

▶

◀

▶

Back

Close

Full Screen / Esc

Printer-friendly Version

Interactive Discussion



1986; Bottenheim et al., 1990, 2009; Sturges et al., 1993; Solberg et al., 1996; Hopper et al., 1998; Ridley et al., 2003; Hirdman et al., 2010). Air masses depleted in O<sub>3</sub> can remain so for several days due to the relatively stable and stratified nature of the Arctic boundary layer (Barrie and Platt, 1997; Stohl, 2006), which limits mixing with surrounding air masses. The most efficient way for an air mass depleted in O<sub>3</sub> to replenish itself is by mixing with O<sub>3</sub> rich air since photochemical O<sub>3</sub> production is generally not sufficient (Simpson et al., 2007b).

The frequently observed low levels of O<sub>3</sub> in the Arctic have been linked to the presence of atomic bromine (Br) radicals (Barrie et al., 1988; Oltmans et al., 1989). It has been posited that Br is responsible for the near complete destruction of surface O<sub>3</sub> on the timescale of about a day by a heterogeneous, photochemical, chain-reaction (Barrie et al., 1988; McConnell et al., 1992). Jobson et al. (1994) showed that the coincidental loss of a series of alkanes during ODEs could be readily explained by atomic chlorine (Cl) radical oxidation. Acetylene was the only hydrocarbon that showed more decay than could be explained by Cl chemistry alone. Br oxidation was invoked in order to fully account for the loss of acetylene in O<sub>3</sub> depleted air masses. These observations directly link the oxidation of volatile organic compounds (VOCs) and surface O<sub>3</sub> destruction to the reactive halogens Br and Cl.

Previous studies have utilized modeled air mass back trajectories in order to identify possible source regions of O<sub>3</sub> depletion chemistry. These studies showed that air masses depleted in O<sub>3</sub> had advected over the predominately ice- and snow-covered Arctic Ocean (Hopper et al., 1998) or over open leads in the sea ice (Sturges et al., 1993). Arctic sea ice can be divided into two main categories: multi-year ice (MYI) and first-year ice (FYI). MYI has survived the annual melt, which typically occurs in September in the Arctic, whereas FYI is formed subsequent to the annual melt. While FYI can eventually evolve into MYI, the two types of ice differ geographically, chemically, and physically. MYI is located primarily in the western Arctic near Greenland and the Canadian archipelago while FYI forms in the eastern (Siberian) Arctic and is transported westward across the pole (Fowler et al., 2004; Belchansky et al., 2005). FYI has been

**Ozone variability and halogen oxidation**

J. B. Gilman et al.

Title Page

Abstract

Introduction

Conclusions

References

Tables

Figures

◀

▶

◀

▶

Back

Close

Full Screen / Esc

Printer-friendly Version

Interactive Discussion



shown to have a higher salinity than MYI particularly during the initial freezing process, which forms a concentrated brine layer at the surface (Notz and Worster, 2008). Additionally, open leads and polynyas, semi-permanent areas of open water surrounded by sea ice, are often associated with areas of FYI because it is thinner and more susceptible to fragmentation by the wind and ocean currents. Open leads and polynyas can be a direct source of sea-salt aerosols or they can be covered by a thin layer of ice allowing for the growth of saline crystals called frost flowers (Martin et al., 1995; Kaleschke et al., 2004). While young sea ice has been implicated in halogen activation and O<sub>3</sub> depletion (Wagner et al., 2001; Simpson et al., 2007a; Bottenheim et al., 2009), MYI has not generally been considered to be a strong source of the reactants required for O<sub>3</sub> destruction chemistry.

A series of field measurements were conducted in spring 2008 as part of POLARCAT (Polar Study using Aircraft, Remote Sensing, Surface Measurements and Models, of Climate, Chemistry, Aerosols, and Transport), which was a large international project conducted during the 2007–2008 International Polar Year. In this work, results from 1) ship-based measurements in the North Atlantic and Arctic Oceans, which focused on the ice- and snow-free regions of the Arctic, 2) airborne measurements over northern Alaska and the frozen Beaufort Sea, and 3) ground-based measurements at Barrow, Alaska, are used to investigate the influence of halogen oxidation on O<sub>3</sub> variability within the Arctic and sub-Arctic. Data from two mid-latitude studies on the Atlantic and Pacific coasts are compared to the Arctic datasets in order to investigate the broader, spatial-scale variations in O<sub>3</sub>.

For the ship-based measurements, the exposure of air masses to FYI, MYI, and total ICE (FYI+MYI) was quantitatively determined by FLEXPART, a Lagrangian particle dispersion model (Stohl et al., 2002, 2005). FLEXPART has been extensively validated (Stohl et al., 1998, 2003) and has been used to investigate long-range transport to the Arctic (Stohl, 2006; Warneke et al., 2009, 2010; Hirdman et al., 2010). The FLEXPART model is used here to determine if the variability in O<sub>3</sub> could be explained by the cumulative exposure to specific types of sea ice.

**Ozone variability and halogen oxidation**

J. B. Gilman et al.

[Title Page](#)[Abstract](#)[Introduction](#)[Conclusions](#)[References](#)[Tables](#)[Figures](#)[◀](#)[▶](#)[◀](#)[▶](#)[Back](#)[Close](#)[Full Screen / Esc](#)[Printer-friendly Version](#)[Interactive Discussion](#)

## 2 Methods

### 2.1 Ship-based measurements in North Atlantic and Arctic Oceans

The International Chemistry Experiment in the Arctic Lower Troposphere (ICEALOT) was conducted aboard the R/V “Knorr” in the North Atlantic and Arctic Oceans in March and April 2008. The cruise track of the R/V “Knorr”, operated by Woods Hole Oceanographic Institution, is shown in Fig. 1 and has been colored by measured O<sub>3</sub> mixing ratios. The cruise has been divided into four areas of study which include the north-eastern United States (NE US, 41° N to 45° N), the sub-Arctic (45° N to 68° N), Arctic (68° N to 80° N), and Iceland (IS, 62° N to 68° N).

A full suite of volatile organic compounds (VOCs), including C<sub>2</sub>–C<sub>6</sub> hydrocarbons, C<sub>2</sub>–C<sub>4</sub> oxygenated VOCs, C<sub>6</sub>–C<sub>9</sub> aromatics, halogenated VOCs, alkyl nitrates, DMS, and acetonitrile, were measured in situ by a custom built, two-channel, gas chromatograph-mass spectrometer (GC-MS). The inlet for the GC-MS consisted of a 30 m unheated Teflon line (6 mm OD), which was positioned on the forward mast of the R/V “Knorr” approximately 25 m above the waterline. Ambient air was pulled continuously at a rate of approximately 7 L min<sup>-1</sup> through the inlet line to the GC-MS. From this sample stream, two ambient air samples were collected simultaneously via cryogenic trapping at a flow rate of 70 sccm for a total of 5 min. Descriptions of the sampling and instrument configurations have been reported elsewhere (Goldan et al., 2004; Gilman et al., 2009); however, subsequent instrument modifications are detailed here.

The original instrument configuration was designed to analyze two samples in parallel utilizing two separate analytical columns and detectors. Channel one (CH1) consisted of an Al<sub>2</sub>O<sub>3</sub> PLOT column with a flame ionization detector (FID), and the second channel (CH2) consisted of a DB-624 column and a linear quadrupole mass spectrometer (Agilent 5973). The instrument has been reconfigured so that the two samples collected in parallel are now analyzed in series on their respective columns by the mass spectrometer alone. This is achieved by holding the CH2 sample in its cryofocus unit an additional 192 s, which allows enough time for the elution and detection of the

Title Page

Abstract

Introduction

Conclusions

References

Tables

Figures

◀

▶

◀

▶

Back

Close

Full Screen / Esc

Printer-friendly Version

Interactive Discussion



**Ozone variability and halogen oxidation**

J. B. Gilman et al.

[Title Page](#)[Abstract](#)[Introduction](#)[Conclusions](#)[References](#)[Tables](#)[Figures](#)[◀](#)[▶](#)[◀](#)[▶](#)[Back](#)[Close](#)[Full Screen / Esc](#)[Printer-friendly Version](#)[Interactive Discussion](#)

CH1 sample. When the analysis of the CH1 sample is near completion, the cryofocus unit on CH2 is flash heated from  $-165^{\circ}\text{C}$  to  $100^{\circ}\text{C}$  in 0.2 s injecting the sample onto the CH2 column. After injection, a 4-way pneumatic valve (Valco Instruments Co. Inc., Houston, TX) switches so that the sample eluting from the CH2 column is now directed to the mass spectrometer while the remaining CH1 carrier gas is vented. The entire sample collection and analysis sequence repeats automatically every 30 min beginning on the hour and half-hour. The detection limits and uncertainties of the VOC measurements detailed in this study are compiled in Table 1. The gas-phase data have been filtered for contamination by the ship itself.

The new analysis scheme provides several advantages over the original instrument configuration. First, the information gained from measuring the unique ion fragments created by electron-impact ionization greatly increases the accuracy of identification and quantification. Compounds were identified by the FID based solely on their retention times and compounds that co-eluted were often difficult to accurately quantify. Secondly, the mass spectrometer is more sensitive to a wider range of species including halocarbons, noble gases, and nitrous oxide ( $\text{N}_2\text{O}$ ). Lastly, all of the data for both channels are now compiled into a single chromatogram. This has increased the efficiency of analyzing the chromatograms, which used to require separate analysis programs and protocols for the two different detectors.

$\text{O}_3$  was measured via UV absorbance by a commercial instrument (Thermo Environmental Instruments, Inc., Model 49c). Carbon monoxide (CO) was measured by a vacuum-UV resonance fluorescence instrument (Gerbig et al., 1999). The  $\text{O}_3$  and CO measurements presented in this analysis represent 5 min averages coincident with the GC-MS sample acquisition. Radon measurements, detailed in Bates et al. (2008), are 30 min averages which overlap with each of the GC-MS samples.

## 2.2 Airborne measurements in Alaskan Arctic

The Aerosol, Radiation, and Cloud Processes affecting Arctic Climate (ARCPAC) campaign was conducted in Fairbanks, Alaska in April 2008 using the NOAA WP-3D

**Ozone variability and halogen oxidation**

J. B. Gilman et al.

Title Page

Abstract

Introduction

Conclusions

References

Tables

Figures

◀

▶

◀

▶

Back

Close

Full Screen / Esc

Printer-friendly Version

Interactive Discussion



aircraft. NOAA whole air samples (NWS) were collected in glass flasks during the research flights that were made over northern Alaska and the frozen Beaufort Sea. The flasks were transported to the NOAA Global Monitoring Division laboratory in Boulder, CO where they were analyzed within a few days for hydrocarbons and halocarbons using GC-MS (Montzka et al., 1993; Warneke et al., 2009). The limit of detection for the VOCs in the NWS is approximately 5 ppt. The NWS acetylene results have been multiplied by a factor of 1.3 so that the acetylene measurements were on a consistent scale with the shipboard in situ GC-MS. The factor of 1.3 is based on measured differences in the calibration standards of acetylene used by the different research groups. We have not attempted to resolve here which standards are more accurate.

During ARCPAC,  $O_3$  was measured with a 50 pptv limit of detection and 4% uncertainty on a 1-s time base using NO-induced chemiluminescence (Ryerson et al., 1998).  $O_3$  mixing ratios were averaged over the NWS collection time, which ranged from 6 to 15 s depending on altitude. In the analysis presented here, only the measurements of acetylene and benzene in the 14 samples that were collected below 1 km in altitude and contained mean CO mixing ratios of less than 190 ppbv. Samples with mean  $CO > 190$  ppbv have been excluded from this analysis as these samples are considered to be significantly above the Arctic springtime background of 160 ppbv (Warneke et al., 2009) due to contributions from biomass burning. Figure 1 shows the sampling locations and the mean  $O_3$  mixing ratios of each of the NWS included in this analysis.

### 2.3 Ground-based measurements in Barrow, AK and Trinidad Head, CA

The Barrow, Alaska Observatory (BRW at  $71.32^\circ N$ ,  $156.61^\circ W$ ) is located approximately 8 m above sea level near the northernmost point of the United States. The prevailing winds at BRW are from the east-northeast off the Beaufort Sea (Oltmans and Levy, 1994). The Observatory at Trinidad Head, California (THD at  $41.05^\circ N$ ,  $124.15^\circ W$ ) is located on the northern coast of California about 100 m above sea level. THD is a relatively remote, mid-latitude, coastal site with prevailing maritime airflow off the Pacific Ocean (Oltmans et al., 2008). Flasks are collected in stainless steel

canisters at both surface sites on a weekly basis year round, but only a subset of those flasks are analyzed for acetylene on the same instrument and by the same procedures as described in Sect. 2.2.

$O_3$  is measured by UV absorption at both surface sites year round (Oltmans and Levy, 1994). The  $O_3$  measurements presented here are hourly averages encompassing the time that each flask was filled. The data collected at the surface sites during January through May of 2008 and January to February of 2009 are included in this analysis. This dataset represents the entire acetylene record at both sites for winter and spring that was available at the time of this analysis.

## 2.4 FLEXPART model description

FLEXPART, a Lagrangian particle dispersion model, differs from traditionally isentropic back trajectories in that thousands of particles are released and subjected to atmospheric dynamics including mean wind fields, convection, and turbulence (Stohl et al., 2002, 2003, 2005, see also <http://transport.nilu.no/flexpart>). For this analysis, each release consisted of 60 000 particles. Releases occurred every 30 min, or sooner if there was a shift in wind direction greater than  $15^\circ$  or if the ship moved more than  $0.18^\circ$  in latitude or longitude, for a total of 1735 releases along the cruise track. The paths of the particles in each release were then tracked for 20 days back in time using the mean winds interpolated from the European Center for Medium-Range Weather Forecasts (ECMWF) operational analyses with  $0.5^\circ \times 0.5^\circ$  resolution. The wind fields were updated every three hours beginning at midnight UTC.

The backward simulations of the paths of the particles were mapped onto a uniform 3-dimensional grid as a function of time since the release. From the particle locations, FLEXPART provides a Potential Emission Sensitivity (PES) function, a so-called source-receptor-relationship (Seibert and Frank, 2004). The PES value (in units of  $\text{sg kg}^{-1}$ ) in a particular grid cell is proportional to the residence time of the particle in that cell (Hirdman et al., 2010). This analysis utilizes the PES value for the footprint layer, which is defined as the lowest 100 m of the atmosphere. All particles that reside

## Ozone variability and halogen oxidation

J. B. Gilman et al.

Title Page

Abstract

Introduction

Conclusions

References

Tables

Figures

◀

▶

◀

▶

Back

Close

Full Screen / Esc

Printer-friendly Version

Interactive Discussion



within this shallow layer are presumed to be in contact with Earth's surface.

The PES values for the footprint layer were then folded with gridded sea ice "emission fluxes." First-year ice (FYI) or multi-year ice (MYI) within a particular grid cell was assigned a unit emission of  $1.0 \text{ kg s}^{-1} \text{ m}^{-2}$ , while grids comprised of open water or land were assigned an emission of  $0.0 \text{ kg s}^{-1} \text{ m}^{-2}$ . The sea ice was classified as FYI or MYI by the procedures outlined in Fowler et al. (2004). The sea ice coverage maps and classifications were updated weekly. The result of folding the footprint PES values with the sea ice "emission fluxes" is a map of the sea ice source contribution (units of  $\text{ppbv m}^{-2}$ ), which depicts the magnitude and location of the particles' exposure to FYI or MYI.

By summing up all the FYI or MYI source contributions from each grid cell and integrating over the grid area, the mixing ratio of an inert FYI or MYI "tracer" (in units of ppbv) can be determined for each release along the ship track for 1 to 20 days prior to the initial release. While the amount of the ice tracer is quantitative and is directly proportional to the time that an air mass was in contact with the specified types of sea ice, the absolute scale is arbitrary due to the fact that a unit emission factor of a fictitious tracer was used. The term "exposure" used throughout this text is defined here as the modeled quantity of the specified type of ice tracer in units of ppbv. Examples of the various FLEXPART model outputs are further discussed in Sect. 3.4.

## 3 Results and discussion

### 3.1 VOC ratios as oxidation markers

Primary oxidants of VOCs in the Arctic springtime include the hydroxyl radical (OH) and the halogen atoms Br and Cl (Jobson et al., 1994). These oxidants determine the chemical lifetimes of VOCs that are emitted or transported into the Arctic. The reactivities of VOCs with OH, Cl, and Br can be used to determine the relative importance of the different oxidants (Jobson et al., 1994; Ramacher et al., 1999; Cavender et al.,

## Ozone variability and halogen oxidation

J. B. Gilman et al.

Title Page

Abstract

Introduction

Conclusions

References

Tables

Figures

◀

▶

◀

▶

Back

Close

Full Screen / Esc

Printer-friendly Version

Interactive Discussion



2008). For example, the propane to i-butane ratio (denoted as [Propane]/[i-Butane]) is used throughout this analysis as a marker for OH oxidation. OH oxidation will cause [Propane]/[i-Butane] to increase because i-butane is oxidized by OH approximately 2.4 times faster than propane based on the reaction rate coefficients listed in Table 1. While  
5 [Propane]/[i-Butane] is sensitive to OH oxidation, it will not be affected by Cl oxidation as propane and i-butane have similar Cl reaction rate coefficients, which only differ by a factor of approximately 1.03.

Cl oxidation is indicated by decreases in [n-Butane]/[i-Butane]. n-Butane reacts 1.4 times faster with Cl than i-butane. This ratio is not sensitive to OH oxidation as both  
10 isomers have similar OH reactivities within a factor of 1.04. Neither of the alkane ratios used as OH or Cl oxidation markers will be affected by Br. Br only reacts at appreciable rates with a select group of VOCs including ethene, acetylene, aldehydes, and some halocarbons. A decrease in [Acetylene]/[Benzene] is used throughout this study as an  
15 indicator of halogen oxidation as acetylene is more readily oxidized by both Br and Cl than benzene.

### 3.2 Description of ICEALOT data subsets

Figure 2a–e shows the time series for wind direction, temperature,  $O_3$  and the VOC ratios used as oxidation markers. At the start of the cruise, the R/V “Knorr” sampled off the northeastern coast of the United States (NE US). Much of the air sampled within  
20 this region is characterized as urban outflow where  $O_3$  was negatively correlated with CO and nitric oxide (NO, not shown) due to NO titration of  $O_3$ . The ship briefly sampled a distinctly different air mass on 25 March 2008. The arrival of this air mass was signaled by an abrupt change in the wind direction, sharp increases in the air temperature and absolute humidity (not shown), and decreases in  $O_3$ , CO, and certain VOCs. This  
25 air mass, determined to be sub-tropical in origin, was transported northward as a result of a mid-latitude cyclone positioned to the southwest of the ship.

VOC ratios are used in this analysis because they are less sensitive to dilution and mixing than the absolute concentrations of individual species. We note that VOC ratios

## Ozone variability and halogen oxidation

J. B. Gilman et al.

Title Page

Abstract

Introduction

Conclusions

References

Tables

Figures

◀

▶

◀

▶

Back

Close

Full Screen / Esc

Printer-friendly Version

Interactive Discussion



can be perturbed by 1) the mixing of air parcels that have been exposed to sources with different emission ratios of the specified hydrocarbons or 2) the mixing of air parcels that underwent vastly different degrees of chemical processing (Parrish et al., 2007). We do not further interpret the fine-scale variabilities of the VOC ratios in the NE US data subset, as the ratios were likely influenced by the mixing of urban or sub-tropical air masses with background air rather than by specific types of oxidation.

The sub-Arctic region is defined here as 45° N to 68° N excluding the Iceland leg shown in Fig. 1. Within the sub-Arctic region, there were distinct decreases in O<sub>3</sub> that were not associated with changes in wind direction, temperature, or CO (Fig. 2). For example, O<sub>3</sub> decreased from 45 to 32 ppbv on 28 March 2008. During this time, there were simultaneous decreases in [Acetylene]/[Benzene] and [n-Butane]/[i-Butane] while [Propane]/[i-Butane] remained constant indicating that this air mass was predominately exposed to halogen oxidation. FLEXPART indicates that this air mass originated in the Arctic before advecting over northeastern Canada, Baffin Bay, and the Davis Strait. Shortly after this period, the path of the air mass shifted from the western (Canadian) Arctic to the eastern (Siberian) Arctic.

A plume enriched in hydrocarbons was encountered on 8 April 2008 as the R/V “Knorr” traveled eastward towards the Norwegian/Russian border. The enrichment of the C3-C5 alkanes, determined by comparing the maximum values listed in italics in Table 1 to their median values, increased according to carbon number and was greater for the linear alkanes compared to their branched isomers. This resulted in the sharp increase in [n-Butane]/[i-Butane] and decrease in [Propane]/[i-Butane] as shown in Fig. 2d and Fig. 2e, respectively. FLEXPART shows that this air mass had advected over the Kola Peninsula near the city of Murmansk, Russia, which represents a local, anthropogenic, point source of VOCs. This source had a distinctive VOC source signature, which resulted in the perturbation of the alkane ratios used as oxidation markers. This plume is likely associated with natural gas processing that is common to the area rather than urban outflow as was observed in the NE US.

A prolonged period of reduced O<sub>3</sub> was observed from 15–20 April 2008 when the

**Ozone variability and halogen oxidation**

J. B. Gilman et al.

Title Page

Abstract

Introduction

Conclusions

References

Tables

Figures

◀

▶

◀

▶

Back

Close

Full Screen / Esc

Printer-friendly Version

Interactive Discussion



ship was near the coast of Svalbard, Norway and in close proximity (0.5 to 2.0 km) to sea ice. During this time, the wind was predominately from the north. The ambient temperature reached a minimum of  $-18^{\circ}\text{C}$ , and  $\text{O}_3$  was reduced from 43 ppbv to 1.5 ppbv as shown in Fig. 2a, b. FLEXPART indicates that the air masses sampled throughout this time period were entirely Arctic in origin, having been confined to latitudes north of  $80^{\circ}\text{N}$  for the majority of their 20-day histories. Because some of the fluctuations in  $\text{O}_3$  correspond to brief changes in the surface wind direction and temperature, it is likely that these observations were of air that had been previously depleted in  $\text{O}_3$  prior to being transported to the R/V “Knorr” rather than active halogen oxidation occurring at the ship’s location. The strong association between the time series of  $\text{O}_3$ , [Acetylene]/[Benzene], and [n-Butane]/[i-Butane], as shown in Fig. 2b–e, indicates that the air mass had been exposed to both Cl and Br oxidation. Lerner et al. (2010) calculated a mean [Br]/[Cl] ratio of  $1600 \pm 200$  during this large-scale ODE. This is consistent with previously reported [Br]/[Cl], which ranges from approximately 400 to 2000 (Jobson et al., 1994; Cavender et al., 2008).

The gradual increase in [Propane]/[i-Butane] from 20 April 2008 to the end of the cruise in Iceland (Fig. 2e) indicates the growing influence of OH chemistry in the Arctic and sub-Arctic in the late spring. During this time period, CO gradually decreased while  $\text{O}_3$  reached a campaign maximum of 51 ppbv. The atmospheric lifetime of CO is largely controlled by reaction with OH, and OH radicals are responsible for the photochemical production of  $\text{O}_3$ . FLEXPART indicates that the air masses sampled during this time had large footprint emission sensitivities to Eastern Europe. The previously noted changes in CO,  $\text{O}_3$ , and the VOC ratios towards the end of the campaign are likely influenced by the mixing of background air in the Arctic with air from more southerly regions where OH oxidation is increasingly important.

### 3.3 Halogen oxidation and $\text{O}_3$ variability

A scatter plot of [Acetylene]/[Benzene] versus  $\text{O}_3$  is used to assess the impact of halogen oxidation on the variability of surface  $\text{O}_3$ . Figure 3a includes the scatter plot for the

15896

ACPD

10, 15885–15919, 2010

## Ozone variability and halogen oxidation

J. B. Gilman et al.

Title Page

Abstract

Introduction

Conclusions

References

Tables

Figures

◀

▶

◀

▶

Back

Close

Full Screen / Esc

Printer-friendly Version

Interactive Discussion



**Ozone variability and halogen oxidation**

J. B. Gilman et al.

Title Page

Abstract

Introduction

Conclusions

References

Tables

Figures

◀

▶

◀

▶

Back

Close

Full Screen / Esc

Printer-friendly Version

Interactive Discussion



ICEALOT data, which have been colored by latitude, as well as the linear regressions and corresponding correlation coefficients for the NE US ( $r=0.30$ ), sub-Arctic ( $r=0.72$ ), and Arctic ( $r=0.98$ ) data subsets. The correlation between [Acetylene]/[Benzene], used here as a marker for Br+Cl oxidation, and  $O_3$  strengthened as the R/V “Knorr” sailed north towards the Arctic. The fit for the Arctic data subset shows a high degree of correlation with  $r=0.98$  for the 544 data points collected north of  $68^\circ N$ . When the analysis is expanded to include the additional 347 data points collected in the sub-Arctic, the correlation for the combined Arctic and sub-Arctic region remains strong with  $r=0.90$ .

The strength of the correlation between [Acetylene]/[Benzene] and  $O_3$  in the Arctic and sub-Arctic is remarkable given that the sources and atmospheric fates of these species are quite different. One factor linking acetylene and  $O_3$  is their common reactivity with Br. The correlation between [Acetylene]/[Benzene] and  $O_3$  indicates that 1) halogen oxidation accounted for up to 96% ( $r=0.98$ ,  $r^2=0.96$ ) of the variability in  $O_3$  measured in the Arctic marine boundary layer in the springtime during ICEALOT and 2) halogen oxidation, which likely occurred in the Arctic high latitudes, influenced  $O_3$  variability in the sub-Arctic.

Figure 3b compares the ICEALOT dataset to other measurements in the Arctic and at coastal mid-latitudes in order to gauge the spatial extent of halogen oxidation influence on surface  $O_3$  variability. The data from two springtime Alaskan studies, AR-CPAC and Barrow, follow the same trend as the ICEALOT data collected on the opposite side of the Arctic. This implies that 1) the relative importance of Br and Cl radical chemistry was similar throughout the Arctic boundary layer during the springtime and 2) any mixing and/or dilution of air masses within the Arctic boundary layer did not perturb the relationship between [Acetylene]/[Benzene] and  $O_3$ . Jobson et al. (1994) suggested that the effects of mixing and dilution of air masses on VOC ratios measured within the Arctic will be minimal because of the narrow range of air mass photochemical ages. In terms of Fig. 3b, halogen chemistry largely determines the slope of the Arctic fit while mixing/transport affects the intensity of the depletion (i.e.,

position along the fitted line) assuming that the oxidation chemistry is no longer active. Background values ( $O_3=43$  ppbv and  $[Acetylene]/[Benzene]=4.0$ ) represent thoroughly mixed air masses whereas the lower values seen in the large-scale ODE ( $O_3=1.5$  ppbv and  $[Acetylene]/[Benzene]=1.0$ ) are associated with lesser degrees of mixing.

5 Measurements from two mid-latitude coastal sites have been added to Fig. 3b for comparison. The New England Air Quality Study (NEAQS) was conducted along the northeastern coast of the US aboard the NOAA R/V “Brown” in the summer of 2004 (Warneke et al., 2007).  $[Acetylene]/[Benzene]$  from NEAQS is comparable to that measured during the springtime ICEALOT cruise in a similar geographic region. However,  $[Acetylene]/[Benzene]$  and  $O_3$  were not significantly correlated in the NE US data subset ( $r^2 = 0.09$ ) or during NEAQS indicating that halogen oxidation was not a large factor in determining  $O_3$  variability in this region in either spring or summer. This is in accordance with the findings of Keene et al. (2007) who determined that Br chemistry is relatively unimportant in the evolution of polluted coastal air in this region.

15 The observatory at Trinidad Head, California (THD) is located along the Pacific coast at approximately the same latitude as the east coast studies (Fig. 1). Oltmans et al. (2008) determined that approximately 25% of the air masses reaching THD in April originate in northern Alaska and are transported at relatively low altitudes throughout their modeled 10-day trajectories. Figure 3b shows that  $[Acetylene]/[Benzene]$  is independent of  $O_3$  at THD in late winter and spring. Even though a fraction of the air masses reaching THD in the spring may have originated the Arctic, there is no indication that  $O_3$ -poor air transported from the Arctic had an appreciable influence on surface  $O_3$  variability at THD for the samples analyzed. We note that  $[Acetylene]/[Benzene]$  is markedly lower for THD compared to the east coast studies. This is attributed to differences in source emission ratios (Warneke et al., 2007; Parrish et al., 2009) and transport patterns (Oltmans et al., 2008) impacting the Atlantic and Pacific Coasts.

**Ozone variability and halogen oxidation**

J. B. Gilman et al.

Title Page

Abstract

Introduction

Conclusions

References

Tables

Figures

◀

▶

◀

▶

Back

Close

Full Screen / Esc

Printer-friendly Version

Interactive Discussion



### 3.4 Modeled sea ice exposure

FLEXPART was used to quantitatively determine the exposure of air masses intercepted by the R/V “Knorr” to first-year ice (FYI), multi-year ice (MYI), and total ICE (FYI+MYI). Examples of the modeling products used to determine the sea ice exposure for the air mass sampled on 2 April 2008 at 00:00 UTC are described here. Gas phase measurements from this period indicate that this air mass was exposed to halogen oxidation (refer to Fig. 2).

A map of the FLEXPART footprint PES, shown in Fig. 4a, identifies where the released particles spent the most amount of time in the lowest 100 m of the atmosphere. The footprint PES map shows that this particular air mass remained largely intact for the first 5 days prior to arrival at the ship’s location, but was broadly dispersed across the eastern Arctic further back in time. A map of the sea ice coverage colored by the modeled sea ice age for the week of 1–7 April 2008 is shown in Fig. 4b. The sea ice coverage was classified as FYI or MYI by the procedures outlined in Fowler et al. (2004).

The exposure of the sampled air mass to FYI or MYI was determined by folding the footprint PES with gridded sea ice coverage, which was assigned a unit emission flux of a FYI or MYI “tracer.” This results in the FYI and MYI source contribution maps shown in Fig. 4c and d, respectively, for the air intercepted on 2 April 2008 at 00:00 UTC. The sea ice source contribution maps (units of ppbv m<sup>-2</sup>) depict the location and magnitude of FYI or MYI contributions to the cumulative ice “tracer” (units of ppbv) encountered by the R/V “Knorr” over the air mass’s 20 day history. The combined maps in Fig. 4 show that this air mass was transported over open water for approximately 3 days prior to sampling, exposed primarily to MYI in the western Arctic for the days 3–5 prior to sampling, and exposed mainly to FYI in the Siberian Arctic for days 5–20 of its modeled history.

The time series of the cumulative 20-day modeled exposure, defined as the amount of the inert ice tracer, to FYI and MYI are shown in Fig. 5a. The two time series

Title Page

Abstract

Introduction

Conclusions

References

Tables

Figures

◀

▶

◀

▶

Back

Close

Full Screen / Esc

Printer-friendly Version

Interactive Discussion



**Ozone variability and halogen oxidation**

J. B. Gilman et al.

[Title Page](#)[Abstract](#)[Introduction](#)[Conclusions](#)[References](#)[Tables](#)[Figures](#)[I◀](#)[▶I](#)[◀](#)[▶](#)[Back](#)[Close](#)[Full Screen / Esc](#)[Printer-friendly Version](#)[Interactive Discussion](#)

are stacked so that the cumulative value is equal to the total ICE exposure, which is shown in Fig. 5b. On average, exposure to FYI accounts for  $68\pm 15\%$  and MYI accounts for  $32\pm 15\%$  of the absolute exposure to total sea ice for the sub-Arctic and Arctic data subsets. This roughly scales with the relative surface areas of the two ice classes (Fig. 4b). As shown in Fig. 5a,  $O_3$  exhibits a clear negative association with modeled ice exposure such that air masses with the greatest ICE exposure had the lowest measured  $O_3$ . Additionally, air masses with the largest depletions in  $O_3$  (e.g., 6–9 April and 15–18 April 2008) have a larger than average contribution from MYI, which accounts for approximately 50–60% of the total ICE exposure for these events.

The time series of the total ICE exposure (Fig. 5b) is colored by the FLEXPART age, which is defined as the number of days backwards in time from the initial release of the particles. This figure shows that a wide range of FLEXPART ages contributed to the modeled ICE exposure. In the sub-Arctic region, air masses show larger contributions from the 5–15 day FLEXPART ages. This is in accordance with the greater time required for air masses exposed to sea ice covering the Arctic Ocean to be transported to latitudes as far south as  $45^\circ$  N. Consistently, the air masses with the largest contribution from 1–5 day FLEXPART ages were encountered in the Arctic when the ship was in close proximity (0.5 to 2.0 km) to sea ice.

The decrease in  $O_3$  on 28 March 2008, previously described in Sect. 3.1 and highlighted in Fig. 2b, corresponds with a sharp increase in the modeled ICE exposure. FLEXPART source contribution maps show that this air mass was in contact with FYI in the Davis Strait and both Hudson and Baffin Bays as recently as 2–3 days prior to being arrival at the R/V “Knorr”, while it required over 10 days of transport for the air mass to be exposed to MYI within the Arctic. This marks the most southerly latitude,  $52^\circ$  N, where an air mass with reduced  $O_3$  due to halogen chemistry could be directly linked to significant exposure to sea ice by FLEXPART.

### 3.5 Correlations between O<sub>3</sub> and modeled sea ice exposure

Correlations between O<sub>3</sub> and the modeled exposure to FYI, MYI, and total ICE is used to determine if the variability in O<sub>3</sub> can be explained by the residence time over these types of sea ice. The depletion of O<sub>3</sub> is used here as a proxy for the presence of reactive halogens; however, the actual amount of O<sub>3</sub> destroyed is dependent on a number of variables including the initial concentration of O<sub>3</sub> within the air mass, the absolute concentrations of the halogens, the relative ratio between Br and Cl, and the reaction time in addition to several other factors. If one type of ice were the dominant source of the reactive halogens responsible for the destruction of O<sub>3</sub> (i.e., a source region of reactive halogens), one would expect to see a stronger correlation between the exposure to that particular type of ice and the amount of O<sub>3</sub> destroyed assuming that all other reaction variables are similar.

The results of the linear correlations between the modeled exposures to FYI, MYI, and ICE versus O<sub>3</sub> are shown in Fig. 6. The correlation coefficients,  $r$ , are plotted as a function of FLEXPART age in Fig. 6a and Fig. 6b for the Arctic and combined Arctic and sub-Arctic data subsets, respectively. The FLEXPART ages are cumulative so that, for example, the modeled exposure on day 5 represents the sum of the exposure for days 1–5 of an air mass's history.

All of the correlations between the modeled sea ice exposures and O<sub>3</sub> are negative indicating that increased exposure to FYI, MYI, or ICE is directly associated with reduced levels of O<sub>3</sub> in the Arctic and sub-Arctic marine boundary layer during the spring. O<sub>3</sub> correlated best with total ICE exposure for both data subsets. A mean correlation coefficient for ICE of  $r = -0.86 \pm 0.03$  ( $r^2 = 0.73$ ) implies that up to 73% of the O<sub>3</sub> variability measured in the Arctic can be related to the modeled exposure to total ICE. As a sensitivity test, the correlation coefficients were also calculated for the same data subsets, but without the large-scale O<sub>3</sub> depletion. The correlation coefficient weakened from  $-0.86$  to  $-0.60$  indicating that this ODE was important but not solely responsible for the observed correlation between O<sub>3</sub> and the modeled ICE exposure.

## Ozone variability and halogen oxidation

J. B. Gilman et al.

Title Page

Abstract

Introduction

Conclusions

References

Tables

Figures

◀

▶

◀

▶

Back

Close

Full Screen / Esc

Printer-friendly Version

Interactive Discussion



**Ozone variability and halogen oxidation**

J. B. Gilman et al.

[Title Page](#)[Abstract](#)[Introduction](#)[Conclusions](#)[References](#)[Tables](#)[Figures](#)[◀](#)[▶](#)[◀](#)[▶](#)[Back](#)[Close](#)[Full Screen / Esc](#)[Printer-friendly Version](#)[Interactive Discussion](#)

There were very few air masses which had significant exposure to FYI within the first 3 days of its transport history resulting in poorer correlation coefficients for these FLEXPART ages. FYI appears to be slightly better correlated with  $O_3$  than MYI for the 4–10 day ages, but the differences between exposure to FYI and MYI are small.

This was partly due to the fact that the exposures to FYI and MYI were generally well correlated with one another ( $0.70 < r < 0.87$ ) indicating that the air masses were sufficiently well dispersed so that they were often in contact with both types of ice at the same time. As a result of this colinearity, the relative importance of exposure to FYI or MYI in determining  $O_3$  variability remains inconclusive for the ICEALOT data set.

### 3.6 Correlations between other gases and modeled sea ice exposure

The modeled sea ice exposure is compared to other trace gases measured aboard the R/V “Knorr”. The linear correlation coefficients for the 6-day cumulative ICE exposure versus various gas-phase measurements made in the Arctic are compiled in Fig. 7. The 6-day ICE exposure was chosen because it represents the shortest amount of time to produce the strongest correlation with  $O_3$  (Fig. 6a).  $O_3$  and the halogen oxidation markers [Acetylene]/[Benzene] and [i-Butane]/[n-Butane] have the strongest negative correlations. This is consistent with the variability of these species being heavily influenced by halogen oxidation. [Acetylene]/[Benzene] has a stronger correlation with ICE exposure than acetylene alone reiterating the facts that 1) destruction of acetylene by halogen oxidation drives the variability of [Acetylene]/[Benzene], and 2) the ratio is less sensitive to the influence of mixing and dilution than the absolute mixing ratio of acetylene alone.

The correlation coefficients for the C2–C6 alkanes are negative and generally increase with increasing carbon number. The oxidation of alkanes by Cl produces aldehydes and ketones, but the differences in the reactivities of these oxidized products with Cl and Br also influence their abundance. Aldehydes are highly reactive with both Cl and Br resulting in their reduction during ODEs on short timescales (Cavender et al., 2008). This is in accordance with the negative correlations of aldehydes with ICE

exposure shown in Fig. 7. Ketones are produced from alkane + Cl reaction faster than they are destroyed by ketone + Cl reaction (Cavender et al., 2008). The net production of ketones from halogen oxidation results in the positive correlation. High concentrations of ketones have also been found in the snow-pack (Domine and Shepson, 2002; Grannas et al., 2002). Emissions of these compounds from the snow would further strengthen the positive correlation between ketones and ICE exposure.

Both radon and dimethyl sulfide (DMS) have weakly negative correlations with ICE exposure, which are qualitatively examined here. Atmospheric sources of radon are land-based whereas DMS is of oceanic origin (Ferek et al., 1995); therefore, the concentrations of these species are expected to be smaller in air masses that have been exposed to ICE rather than land or open water. Conversely, trace gases with atmospheric sinks other than ICE should exhibit positive correlations. The more time that an air parcel is exposed to sea ice, the lower the possibility of surface uptake by exposure to open water or land. This is true for acetonitrile, which has an oceanic sink (de Gouw et al., 2003; Jost et al., 2003). Benzene, CO, and [Propane]/[i-Butane], which is used here as an OH oxidation marker, have no correlation with ICE exposure ( $r < 0.05$ ). Compounds like benzene and CO have relatively long atmospheric lifetimes, are not sensitive to halogen oxidation, and do not have strong sources or sinks within the ice- and snow-covered Arctic.

Bromoform ( $\text{CHBr}_3$ ) exhibits the strongest positive correlation with ICE exposure. Like DMS,  $\text{CHBr}_3$  has known oceanic sources (Cota and Sturges, 1997). If the presence of  $\text{CHBr}_3$  is simply due to its oceanic source, it would be expected to have a negative correlation as does DMS even though the sources of DMS and  $\text{CHBr}_3$  within the ocean can be quite different. The strong positive correlation between  $\text{CHBr}_3$  and the modeled ICE exposure suggests that sea ice is possibly a direct source of  $\text{CHBr}_3$  and/or  $\text{CHBr}_3$  may be produced during  $\text{O}_3$  depletion chemistry.

**Ozone variability and halogen oxidation**

J. B. Gilman et al.

Title Page

Abstract

Introduction

Conclusions

References

Tables

Figures

◀

▶

◀

▶

Back

Close

Full Screen / Esc

Printer-friendly Version

Interactive Discussion



## 4 Summary

The influence of halogen oxidation on the variability of O<sub>3</sub> and VOCs in the Arctic and sub-Arctic boundary layer was investigated using field measurements from multiple studies conducted in March and April 2008 as part of the POLARCAT project.

5 Ship-based measurements conducted in the ice-free regions of the North Atlantic and Arctic Oceans significantly expanded upon the existing spatial and temporal database of VOCs in the Arctic and sub-Arctic springtime marine boundary layer. The wide geographic area sampled by the ship provided unique insights on the influence of halogen destruction of surface O<sub>3</sub> in the northern high latitudes and the transport of O<sub>3</sub>-poor air masses from the Arctic Basin to latitudes as far south as 52° N.

10 The VOC ratios [Propane]/[i-Butane], [n-Butane]/[i-Butane], and [Acetylene]/[Benzene] were used as markers for of OH, Cl, and Br+Cl oxidation, respectively. The correlation between [Acetylene]/[Benzene] and O<sub>3</sub> was used to assess the influence of halogen oxidation on surface O<sub>3</sub> variability. This correlation strengthened as the R/V “Knorr” sailed northward towards the Arctic. O<sub>3</sub> was highly correlated with [Acetylene]/[Benzene] with  $r=0.98$  for the 544 data points collected north of 68° N suggesting that halogen oxidation accounted for up to 96% of the variability in O<sub>3</sub> measured in the springtime Arctic marine boundary layer during this study.

15 The strong correlation between [Acetylene]/[Benzene] and O<sub>3</sub> observed aboard the ship was substantiated by concurrent airborne and ground-based measurements within the Alaskan Arctic. This implies that 1) the oxidation chemistry was similar throughout the Arctic boundary layer in the springtime and 2) the mixing and dilution of air masses within the Arctic surface layer did not significantly perturb the correlation between [Acetylene]/[Benzene] and O<sub>3</sub>. The analysis was further expanded to include the sub-Arctic (45° N to 68° N) and two coastal mid-latitude sites (~40° N) in order to investigate the broader, spatial-scale variations in O<sub>3</sub>. The results of this analysis indicated that halogen oxidation, which likely occurred in the Arctic high latitudes, influenced O<sub>3</sub> variability in the sub-Arctic; however, this influence did not extend to either of the

### Ozone variability and halogen oxidation

J. B. Gilman et al.

Title Page

Abstract

Introduction

Conclusions

References

Tables

Figures

◀

▶

◀

▶

Back

Close

Full Screen / Esc

Printer-friendly Version

Interactive Discussion



coastal mid-latitude sites. The potential of this influence of Arctic air on more southerly latitudes warrants further investigation.

FLEXPART, a Lagrangian particle dispersion model, was used to quantitatively determine the exposure of air masses intercepted by the ship to first-year ice (FYI), multi-year ice (MYI), and ICE (FYI+MYI). The modeled sea ice exposure was negatively correlated with O<sub>3</sub> indicating that increased exposure to Arctic sea ice was associated with reduced levels of O<sub>3</sub> in the Arctic and sub-Arctic marine boundary layer during this springtime study. The modeled ICE exposure was compared to other gases measured aboard the R/V "Knorr" in order to demonstrate that the model is sensitive to the source region where halogen oxidation chemistry occurs.

*Acknowledgements.* The authors would like to thank the crew members and fellow scientists aboard the R/V "Knorr" and the NOAA WP-3D for their help and expertise. The radon measurements aboard the R/V "Knorr" were provided by J. E. Johnson and T. S. Bates of NOAA's Pacific Marine Environmental Laboratory. The authors thank the station personnel responsible for filling flasks and overseeing the O<sub>3</sub> monitors at BRW and THD. Results from BRW, THD, and from the NWS during ARCPAC were supported in part by the Atmospheric Composition and Climate Program of NOAA's Climate Program Office. Support of the FLEXPART analysis for this study was provided by the Norwegian Research Council through the POLARCAT project (NFR#175916).

## References

- Atkinson, R. and Aschmann, S. A.: Kinetics of the gas phase reaction of Cl atoms with a series of organics at 296 +/- 2K and atmospheric pressure, *Int. J. Chem. Kinet.*, 17, 33–41, 1985.
- Atkinson, R.: Kinetics and mechanisms of the gas-phase reactions of the hydroxyl radical with organic-compounds under atmospheric conditions, *Chem. Rev.*, 86, 69–201, 1986.
- Atkinson, R., Baulch, D. L., Cox, R. A., Crowley, J. N., Hampson, J. R. F., Kerr, J. A., Rossi, M. J., and Troe, J.: Summary of evaluated kinetic and photochemical data for atmospheric chemistry, IUPAC Gas Kinetic Data Evalu. for Atmos. Chem., Web Version December 2001, 1–56, 2001.

## Ozone variability and halogen oxidation

J. B. Gilman et al.

Title Page

Abstract

Introduction

Conclusions

References

Tables

Figures

◀

▶

◀

▶

Back

Close

Full Screen / Esc

Printer-friendly Version

Interactive Discussion



**Ozone variability and  
halogen oxidation**

J. B. Gilman et al.

Title Page

Abstract

Introduction

Conclusions

References

Tables

Figures

◀

▶

◀

▶

Back

Close

Full Screen / Esc

Printer-friendly Version

Interactive Discussion



- Atkinson, R.: Kinetics of the gas-phase reactions of OH radicals with alkanes and cycloalkanes, *Atmos. Chem. Phys.*, 3, 2233–2307, doi:10.5194/acp-3-2233-2003, 2003.
- Barrie, L. and Platt, U.: Arctic tropospheric chemistry: an overview, *Tellus B*, 49, 450–454, 1997.
- 5 Barrie, L. A., Bottenheim, J. W., Schnell, R. C., Crutzen, P. J., and Rasmussen, R. A.: Ozone destruction and photochemical reactions at polar sunrise in the lower Arctic atmosphere, *Nature*, 334, 138–141, 1988.
- Bates, T. S., Quinn, P. K., Coffman, D., Schulz, K., Covert, D. S., Johnson, J. E., Williams, E. J., Lerner, B. M., Angevine, W. M., Tucker, S. C., Brewer, W. A., and Stohl, A.: Boundary layer  
10 aerosol chemistry during TexAQS/GoMACCS 2006: Insights into aerosol sources and transformation processes, *J. Geophys. Res.-Atmos.*, 113, D00F01, doi:10.1029/2008jd010023, 2008.
- Belchansky, G. I., Douglas, D. C., and Platonov, N. G.: Spatial and temporal variations in the age structure of Arctic sea ice, *Geophys. Res. Lett.*, 32, L18504, doi:10.1029/2005gl023976, 15 2005.
- Bottenheim, J. W., Barrie, L. A., Atlas, E., Heidt, L. E., Niki, H., Rasmussen, R. A., and Shepson, P. B.: Depletion of lower tropospheric ozone during Arctic spring – The Polar Sunrise Experiment 1988, *J. Geophys. Res.-Atmos.*, 95, 18555–18568, 1990.
- Bottenheim, J. W., Netcheva, S., Morin, S., and Nghiem, S. V.: Ozone in the boundary layer air  
20 over the Arctic Ocean: measurements during the TARA transpolar drift 2006/2008, *Atmos. Chem. Phys.*, 9, 4545–4557, doi:10.5194/acp-9-4545-2009, 2009.
- Cavender, A. E., Biesenthal, T. A., Bottenheim, J. W., and Shepson, P. B.: Volatile organic compound ratios as probes of halogen atom chemistry in the Arctic, *Atmos. Chem. Phys.*, 8, 1737–1750, doi:10.5194/acp-8-1737-2008, 2008.
- 25 Cota, G. F. and Sturges, W. T.: Biogenic bromine production in the Arctic, *Mar. Chem.*, 56, 181–192, 1997.
- Cuevas, C. A., Notario, A., Martinez, E., and Albaladejo, J.: Temperature-dependence study of the gas-phase reactions of atmospheric Cl atoms with a series of aliphatic aldehydes, *Atmos. Environ.*, 40, 3845–3854, doi:10.1016/j.atmosenv.2006.03.001, 2006.
- 30 de Gouw, J. A., Goldan, P. D., Warneke, C., Kuster, W. C., Roberts, J. M., Marchewka, M., Bertman, S. B., Pszenny, A. A. P., and Keene, W. C.: Validation of proton transfer reaction-mass spectrometry (PTR-MS) measurements of gas-phase organic compounds in the atmosphere during the New England Air Quality Study (NEAQS) in 2002, *J. Geophys. Res.-Atmos.*, 108,

**Ozone variability and halogen oxidation**

J. B. Gilman et al.

[Title Page](#)[Abstract](#)[Introduction](#)[Conclusions](#)[References](#)[Tables](#)[Figures](#)[◀](#)[▶](#)[◀](#)[▶](#)[Back](#)[Close](#)[Full Screen / Esc](#)[Printer-friendly Version](#)[Interactive Discussion](#)

4682, doi:10.1029/2003jd003863 2003.

DeMore, W. B., Sander, S. P., Golden, D. M., Hampson, R. F., Kurylo, M. J., Howard, C. J., Ravishankara, A. R., Kolb, C. E., and Molina, M. J.: Chemical kinetics and photochemical data for use in stratospheric modeling, Evaluation number 12, JPL Pub., 1–266, 1997.

5 Domine, F. and Shepson, P. B.: Air-snow interactions and atmospheric chemistry, *Science*, 297, 1506–1510, 2002.

Ferek, R. J., Hobbs, P. V., Radke, L. F., Herring, J. A., Sturges, W. T., and Cota, G. F.: Dimethyl sulfide in the arctic atmosphere, *J. Geophys. Res.-Atmos.*, 100, 26093–26104, 1995.

10 Fowler, C., Emery, W. J., and Maslanik, J.: Satellite-derived evolution of Arctic sea ice age: October 1978 to March 2003, *IEEE Geosci. Remote S.*, 1, 71–74, doi:10.1109/lgrs.2004.824741, 2004.

Gerbig, C., Schmitgen, S., Kley, D., Volz-Thomas, A., Dewey, K., and Haaks, D.: An improved fast-response vacuum-UV resonance fluorescence CO instrument, *J. Geophys. Res.-Atmos.*, 104, 1699–1704, 1999.

15 Gilman, J. B., Kuster, W. C., Goldan, P. D., Herndon, S. C., Zahniser, M. S., Tucker, S. C., Brewer, W. A., Lerner, B. M., Williams, E. J., Harley, R. A., Fehsenfeld, F. C., Warneke, C., and de Gouw, J. A.: Measurements of volatile organic compounds during the 2006 Tex-AQS/GoMACCS campaign: Industrial influences, regional characteristics, and diurnal dependencies of the OH reactivity, *J. Geophys. Res.*, 114, D00F06, doi:10.1029/2008jd011525, 2009.

20 Goldan, P. D., Kuster, W. C., Williams, E., Murphy, P. C., Fehsenfeld, F. C., and Meagher, J.: Nonmethane hydrocarbon and oxy hydrocarbon measurements during the 2002 New England Air Quality Study, *J. Geophys. Res.-Atmos.*, 109, D21309, doi:10.1029/2003JD004455, 2004.

25 Grannas, A. M., Shepson, P. B., Guimbaud, C., Sumner, A. L., Albert, M., Simpson, W., Domine, F., Boudries, H., Bottenheim, J., Beine, H. J., Honrath, R., and Zhou, X. L.: A study of photochemical and physical processes affecting carbonyl compounds in the Arctic atmospheric boundary layer, *Atmos. Environ.*, 36, 2733–2742, 2002.

30 Hirdman, D., Sodemann, H., Eckhardt, S., Burkhardt, J. F., Jefferson, A., Mefford, T., Quinn, P. K., Sharma, S., Strm, J., and Stohl, A.: Source identification of short-lived air pollutants in the Arctic using statistical analysis of measurement data and particle dispersion model output, *Atmos. Chem. Phys.*, 10, 669–693, doi:10.5194/acp-10-669-2010, 2010.

Hopper, J. F., Barrie, L. A., Silis, A., Hart, W., Gallant, A. J., and Dryfhout, H.: Ozone and me-

**Ozone variability and  
halogen oxidation**

J. B. Gilman et al.

[Title Page](#)[Abstract](#)[Introduction](#)[Conclusions](#)[References](#)[Tables](#)[Figures](#)[◀](#)[▶](#)[◀](#)[▶](#)[Back](#)[Close](#)[Full Screen / Esc](#)[Printer-friendly Version](#)[Interactive Discussion](#)

teorology during the 1994 Polar Sunrise Experiment, *J. Geophys. Res.-Atmos.*, 103, 1481–1492, 1998.

Jobson, B. T., Niki, H., Yokouchi, Y., Bottenheim, J., Hopper, F., and Leaitch, R.: Measurements of C2-C6 hydrocarbons during the Ploar Sunrise 1992 Experiment – Evidence for Cl and Br atom chemistry, *J. Geophys. Res.-Atmos.*, 99, 25355–25368, 1994.

Jost, C., Trentmann, J., Sprung, D., Andreae, M. O., and Dewey, K.: Deposition of acetonitrile to the Atlantic Ocean off Namibia and Angola and its implications for the atmospheric budget of acetonitrile, *Geophys. Res. Lett.*, 30, 1837, doi:10.1029/2003gl017347, 2003.

Kaleschke, L., Richter, A., Burrows, J., Afe, O., Heygster, G., Notholt, J., Rankin, A. M., Roscoe, H. K., Hollwedel, J., Wagner, T., and Jacobi, H. W.: Frost flowers on sea ice as a source of sea salt and their influence on tropospheric halogen chemistry, *Geophys. Res. Lett.*, 31, L16114, doi:10.1029/2004gl020655, 2004.

Kamboures, M. A., Hansen, J. C., and Francisco, J. S.: A study of the kinetics and mechanisms involved in the atmospheric degradation of bromoform by atomic chlorine, *Chem. Phys. Lett.*, 353, 335–344, 2002.

Keene, W. C., Stutz, J., Pszenny, A. A. P., Maben, J. R., Fischer, E. V., Smith, A. M., von Glasow, R., Pechtl, S., Sive, B. C., and Varner, R. K.: Inorganic chlorine and bromine in coastal New England air during summer, *J. Geophys. Res.-Atmos.*, 112, D10S12, doi:10.1029/2006jd007689, 2007.

Lerner, B. M., Gilman, J. B., Murphy, P. C., Kuster, W. C., Johnson, J. E., Bates, T. S., Burkhardt, J. F., de Gouw, J. A., and Williams, E. J.: Observation and characterization of ozone depletion events in the Arctic Ocean during ICEALOT, *Atmos. Chem. Phys. Discuss.*, in preparation, 2010.

Martin, S., Drucker, R., and Fort, M.: A laboratory study of frost flower growth on the surface of young sea ice, *J. Geophys. Res.-Oceans*, 100, 7027–7036, 1995.

McConnell, J. C., Henderson, G. S., Barrie, L., Bottenheim, J., Niki, H., Langford, C. H., and Templeton, E. M. J.: Photochemical bromine production implicated in Arctic boundary layer ozone depletion, *Nature*, 355, 150–152, 1992.

Montzka, S. A., Myers, R. C., Butler, J. H., Elkins, J. W., and Cummings, S. O.: Global tropospheric distribution and calibration scale of HCFC-22, *Geophys. Res. Lett.*, 20, 703–706, 1993.

Notz, D. and Worster, M. G.: In situ measurements of the evolution of young sea ice, *J. Geophys. Res.-Oceans*, 113, C03001, doi:10.1029/2007jc004333, 2008.

**Ozone variability and halogen oxidation**

J. B. Gilman et al.

Title Page

Abstract

Introduction

Conclusions

References

Tables

Figures

◀

▶

◀

▶

Back

Close

Full Screen / Esc

Printer-friendly Version

Interactive Discussion



- Oltmans, S. J. and Komhyr, W. D.: Surface ozone distributions and variations from 1973–1984 Measurements at the NOAA Geophysical Monitoring for Climatic-Change Base-line Observatories, *J. Geophys. Res.-Atmos.*, 91, 5229–5236, 1986.
- Oltmans, S. J., Schnell, R. C., Sheridan, P. J., Peterson, R. E., Li, S. M., Winchester, J. W., Tans, P. P., Sturges, W. T., Kahl, J. D., and Barrie, L. A.: Seasonal surface ozone and filterable bromine relationship in the high Arctic, *Atmos. Environ.*, 23, 2431–2441, 1989.
- Oltmans, S. J. and Levy, H.: Surface ozone measurements from a global network, *Atmos. Environ.*, 28, 9–24, 1994.
- Oltmans, S. J., Lefohn, A. S., Harris, J. M., and Shadwick, D. S.: Background ozone levels of air entering the west coast of the US and assessment of longer-term changes, *Atmos. Environ.*, 42, 6020–6038, doi:10.1016/j.atmosenv.2008.03.034, 2008.
- Parrish, D. D., Stohl, A., Forster, C., Atlas, E. L., Blake, D. R., Goldan, P. D., Kuster, W. C., and de Gouw, J. A.: Effects of mixing on evolution of hydrocarbon ratios in the troposphere, *J. Geophys. Res.-Atmos.*, 112, D10S34, 11–17, doi:10.1029/2006jd007583, 2007.
- Parrish, D. D., Kuster, W. C., Shao, M., Yokouchi, Y., Kondo, Y., Goldan, P. D., de Gouw, J. A., Koike, M., and Shirai, T.: Comparison of air pollutant emissions among mega-cities, *Atmos. Environ.*, 43, 6435–6441, 10.1016/j.atmosenv.2009.06.024, 2009.
- Ramacher, B., Rudolph, J., and Koppmann, R.: Hydrocarbon measurements during tropospheric ozone depletion events: Evidence for halogen atom chemistry, *J. Geophys. Res.-Atmos.*, 104, 3633–3653, 1999.
- Ramacher, B., Orlando, J. J., and Tyndall, G. S.: Temperature-dependent rate coefficient measurements for the reaction of bromine atoms with a series of aldehydes, *Int. J. Chem. Kinet.*, 32, 460–465, 2000.
- Ridley, B. A., Atlas, E. L., Montzka, D. D., Browell, E. V., Cantrell, C. A., Blake, D. R., Blake, N. J., Cinquini, L., Coffey, M. T., Emmons, L. K., Cohen, R. C., DeYoung, R. J., Dibb, J. E., Eisele, F. L., Flocke, F. M., Fried, A., Grahek, F. E., Grant, W. B., Hair, J. W., Hannigan, J. W., Heikes, B. J., Lefer, B. L., Mauldin, R. L., Moody, J. L., Shetter, R. E., Snow, J. A., Talbot, R. W., Thornton, J. A., Walega, J. G., Weinheimer, A. J., Wert, B. P., and Wimmers, A. J.: Ozone depletion events observed in the high latitude surface layer during the TOPSE aircraft program, *J. Geophys. Res.-Atmos.*, 108, 8356, doi:10.1029/2001jd001507, 2003.
- Ryerson, T. B., Buhr, M. P., Frost, G. J., Goldan, P. D., Holloway, J. S., Hubler, G., Jobson, B. T., Kuster, W. C., McKeen, S. A., Parrish, D. D., Roberts, J. M., Sueper, D. T., Trainer, M., Williams, J., and Fehsenfeld, F. C.: Emissions lifetimes and ozone formation in power plant

**Ozone variability and  
halogen oxidation**

J. B. Gilman et al.

Title Page

Abstract

Introduction

Conclusions

References

Tables

Figures

◀

▶

◀

▶

Back

Close

Full Screen / Esc

Printer-friendly Version

Interactive Discussion



- plumes, *J. Geophys. Res.-Atmos.*, 103, 22569–22583, 1998.
- Seibert, P. and Frank, A.: Source-receptor matrix calculation with a Lagrangian particle dispersion model in backward mode, *Atmos. Chem. Phys.*, 4, 51–63, doi:10.5194/acp-4-51-2004, 2004.
- 5 Simpson, W. R., Carlson, D., Hönninger, G., Douglas, T. A., Sturm, M., Perovich, D., and Platt, U.: First-year sea-ice contact predicts bromine monoxide (BrO) levels at Barrow, Alaska better than potential frost flower contact, *Atmos. Chem. Phys.*, 7, 621–627, doi:10.5194/acp-7-621-2007, 2007a.
- 10 Simpson, W. R., von Glasow, R., Riedel, K., Anderson, P., Ariya, P., Bottenheim, J., Burrows, J., Carpenter, L. J., Frieß, U., Goodsite, M. E., Heard, D., Hutterli, M., Jacobi, H.-W., Kaleschke, L., Neff, B., Plane, J., Platt, U., Richter, A., Roscoe, H., Sander, R., Shepson, P., Sodeau, J., Steffen, A., Wagner, T., and Wolff, E.: Halogens and their role in polar boundary-layer ozone depletion, *Atmos. Chem. Phys.*, 7, 4375–4418, doi:10.5194/acp-7-4375-2007, 2007b.
- 15 Solberg, S., Schmidbauer, N., Semb, A., Stordal, F., and Hov, O.: Boundary-layer ozone depletion as seen in the Norwegian Arctic in Spring, *J. Atmos. Chem.*, 23, 301–332, 1996.
- Stohl, A., Hittenberger, M., and Wotawa, G.: Validation of the Lagrangian particle dispersion model FLEXPART against large-scale tracer experiment data, *Atmos. Environ.*, 32, 4245–4264, 1998.
- 20 Stohl, A., Eckhardt, S., Forster, C., James, P., Spichtinger, N., and Seibert, P.: A replacement for simple back trajectory calculations in the interpretation of atmospheric trace substance measurements, *Atmos. Environ.*, 36, 4635–4648, 2002.
- Stohl, A., Forster, C., Eckhardt, S., Spichtinger, N., Huntrieser, H., Heland, J., Schlager, H., Wilhelm, S., Arnold, F., and Cooper, O.: A backward modeling study of intercontinental pollution transport using aircraft measurements, *J. Geophys. Res.-Atmos.*, 108, 4370, doi:10.1029/2002jd002862, 2003.
- 25 Stohl, A., Forster, C., Frank, A., Seibert, P., and Wotawa, G.: Technical note: The Lagrangian particle dispersion model FLEXPART version 6.2, *Atmos. Chem. Phys.*, 5, 2461–2474, doi:10.5194/acp-5-2461-2005, 2005.
- Stohl, A.: Characteristics of atmospheric transport into the Arctic troposphere, *J. Geophys. Res.-Atmos.*, 111, D11306, doi:10.1029/2005jd006888, 2006.
- 30 Sturges, W. T., Schnell, R. C., Landsberger, S., Oltmans, S. J., Harris, J. M., and Li, S. M.: Chemical and meteorological influences on surface ozone destruction at Barrow, Alaska, during Spring 1989, *Atmos. Environ.*, 27, 2851–2863, 1993.

**Ozone variability and  
halogen oxidation**

J. B. Gilman et al.

Title Page

Abstract

Introduction

Conclusions

References

Tables

Figures

◀

▶

◀

▶

Back

Close

Full Screen / Esc

Printer-friendly Version

Interactive Discussion



Wagner, T., Leue, C., Wenig, M., Pfeilsticker, K., and Platt, U.: Spatial and temporal distribution of enhanced boundary layer BrO concentrations measured by the GOME instrument aboard ERS-2, *J. Geophys. Res.-Atmos.*, 106, 24225–24235, 2001.

Wallington, T. J. and Kurylo, M. J.: The gas-phase reactions of hydroxyl radicals with a series of aliphatic alcohols over the temperature range 240–440 K, *Int. J. Chem. Kinet.*, 19, 1015–1023, 1987.

Wallington, T. J., Skewes, L. M., and Siegl, W. O.: Kinetics of the gas-phase reaction of chlorine atoms with a series of alkenes, alkynes and aromatic species at 298 K, *J. Photoch. Photobio. A*, 45, 167–175, 1988.

Wallington, T. J., Skewes, L. M., Siegl, W. O., and Japar, S. M.: A relative rate study of the reaction of bromine atoms with a variety of organic compounds at 298 K, *Int. J. Chem. Kinet.*, 21, 1069–1076, 1989.

Warneke, C., McKeen, S. A., de Gouw, J. A., Goldan, P. D., Kuster, W. C., Holloway, J. S., Williams, E. J., Lerner, B. M., Parrish, D. D., Trainer, M., Fehsenfeld, F. C., Kato, S., Atlas, E. L., Baker, A., and Blake, D. R.: Determination of urban volatile organic compound emission ratios and comparison with an emissions database, *J. Geophys. Res.-Atmos.*, 112, D10S47, doi:10.1029/2006jd007930, 2007.

Warneke, C., Bahreini, R., Brioude, J., Brock, C. A., de Gouw, J. A., Fahey, D. W., Froyd, K. D., Holloway, J. S., Middlebrook, A., Miller, L., Montzka, S., Murphy, D. M., Peischl, J., Ryerson, T. B., Schwarz, J. P., Spackman, J. R., and Veres, P.: Biomass burning in Siberia and Kazakhstan as an important source for haze over the Alaskan Arctic in April 2008, *Geophys. Res. Lett.*, 36, L02813, doi:10.1029/2008gl036194, 2009.

Warneke, C., Froyd, K. D., Brioude, J., Bahreini, R., Brock, C. A., Cozic, J., de Gouw, J. A., Fahey, D. W., Ferrare, R., Holloway, J. S., Middlebrook, A. M., Miller, L., Montzka, S., Schwarz, J. P., Sodemann, H., Spackman, J. R., and Stohl, A.: An important contribution to springtime Arctic aerosol from biomass burning in Russia, *Geophys. Res. Lett.*, 37, L01801, doi:10.1029/2009gl041816, 2010.

Zhao, Z., Huskey, D. T., Nicovich, J. M., and Wine, P. H.: Temperature-dependent kinetics study of the gas-phase reactions of atomic chlorine with acetone, 2-butanone, and 3-pentanone, *Int. J. Chem. Kinet.*, 40, 259–267, doi:10.1002/kin.20321, 2008.

## Ozone variability and halogen oxidation

J. B. Gilman et al.

**Table 1.** Summary of the measurement parameters, statistics, and reaction rate coefficients for OH ( $k_{\text{OH}}$ ), Cl ( $k_{\text{Cl}}$ ), and Br ( $k_{\text{Br}}$ ) with a select group of VOCs measured during ICEALOT. The mean, median, maximum, and minimum values are for the 891 VOC samples in the sub-Arctic and Arctic.

Compound	LOD ppb	Precision	Accuracy	Mean ppb	Median ppb	Max ppb	Min ppb	$k_{\text{OH}}$ at 250 K $10^{12} \text{ cm}^3 \text{ s}^{-1}$	$k_{\text{Cl}}$ at 250 K $10^{12} \text{ cm}^3 \text{ s}^{-1}$	$k_{\text{Br}}$ at 250 K $10^{12} \text{ cm}^3 \text{ s}^{-1}$
Ethane	0.0100	8%	15%	1.694	1.731	2.145	0.976	0.12 [A]	55.6 [A]	NR
Propane	0.0100	6%	15%	0.654	0.682	<i>1.289</i>	<b>0.176</b>	0.72 [A]	141 [A]	NR
i-Butane	0.0050	5%	15%	0.106	0.100	<i>0.309</i>	<b>0.028</b>	1.71 [B]	137 [F*]	NR
n-Butane	0.0050	5%	15%	0.182	0.190	<i>0.941</i>	<b>0.027</b>	1.78 [B]	198 [F*]	NR
i-Pentane	0.0010	5%	20%	0.056	0.058	<i>0.392</i>	<b>0.008</b>	3.60 [B*]	203 [F*]	NR
n-Pentane	0.0010	5%	20%	0.051	0.051	<i>0.441</i>	<b>0.006</b>	2.96 [B]	311 [G*]	NR
n-Hexane	0.0010	5%	20%	0.011	0.012	<i>0.116</i>	<b>0.001</b>	5.2 [B*]	345 [G*]	NR
Acetylene	0.0100	10%	20%	0.365	0.376	0.562	<b>0.071</b>	0.78 [C*]	71 [G*]	0.005 [K*]
Benzene	0.0005	3%	20%	0.097	0.099	0.127	0.054	0.91 [C]	4.0 [G*]	NR
Acetaldehyde	0.0010	15%	25%	0.065	0.056	0.334	<b>0.004</b>	19.1 [A]	72 [A]	3.08 [K]
Propanal	0.0010	15%	25%	0.029	0.023	0.189	<b>0.005</b>	25.8 [A]	120 [A*]	9.73 [K*]
Butanal	0.0010	15%	25%	0.013	0.009	0.130	<b>0.002</b>	30.9 [A]	137 [H*]	20 [L]
Acetone	0.0100	15%	25%	0.476	0.473	0.962	0.158	0.14 [D]	1.42 [I]	NR
2-Butanone	0.0100	15%	25%	0.070	0.068	0.317	0.025	1.17 [A]	37.5 [I]	NR
Bromoform	0.0005	10%	20%	0.002	0.002	<b>0.004</b>	0.001	0.12 [E]	0.22 [J*]	NR

LOD = Limit of detection; Precision = Reproducibility

Italic = Associated with Kola Peninsula plume sampled on 8 April 2008

Bold = Associated with ozone depletion event sampled 15–20 April 2008

[A] = Atkinson et al. (2001); [B] = Atkinson et al. (2003); [C] = Atkinson (1986); [D] = Wallington and Kurylo (1987); [E] = DeMore et al. (1997); [F] = Atkinson and Aschmann (1985); [G] = Wallington et al. (1988); [H] = Cuevas et al. (2006); [I] = Zhao et al. (2008); [J] = Kamboures et al. (2002); [K] = Wallington et al. (1989); [L] = Ramancher et al. (2000); NR = Negligible Reactivity

\* denotes rate coefficients at 298 K

Title Page

Abstract

Introduction

Conclusions

References

Tables

Figures

◀

▶

◀

▶

Back

Close

Full Screen / Esc

Printer-friendly Version

Interactive Discussion



Ozone variability and  
halogen oxidation

J. B. Gilman et al.

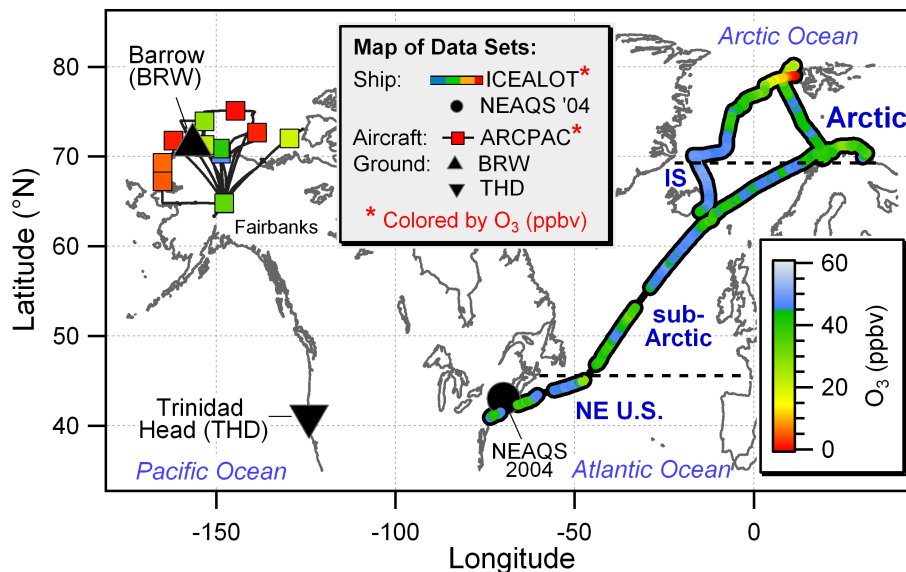


**Fig. 1.** Locations of the data sets used in this analysis. The four data subsets of the ICEALOT campaign aboard the R/V “Knorr”, which include the northeastern United States (NE US), sub-Arctic, Arctic, and Iceland (IS), are identified. The ICEALOT ship track and the flask samples collected along the ARCPAC flight tracks in Northern Alaska are colored by measured O<sub>3</sub> mixing ratios. Additional data sets include flask samples collected at ground-based observatories in Barrow, Alaska (BRW) and Trinidad Head, California (THD) as well as ship-based studies from the 2004 New England Air Quality Study (NEAQS '04) aboard the R/V “Brown”.

Title Page

Abstract

Introduction

Conclusions

References

Tables

Figures

◀

▶

◀

▶

Back

Close

Full Screen / Esc

Printer-friendly Version

Interactive Discussion



## Ozone variability and halogen oxidation

J. B. Gilman et al.

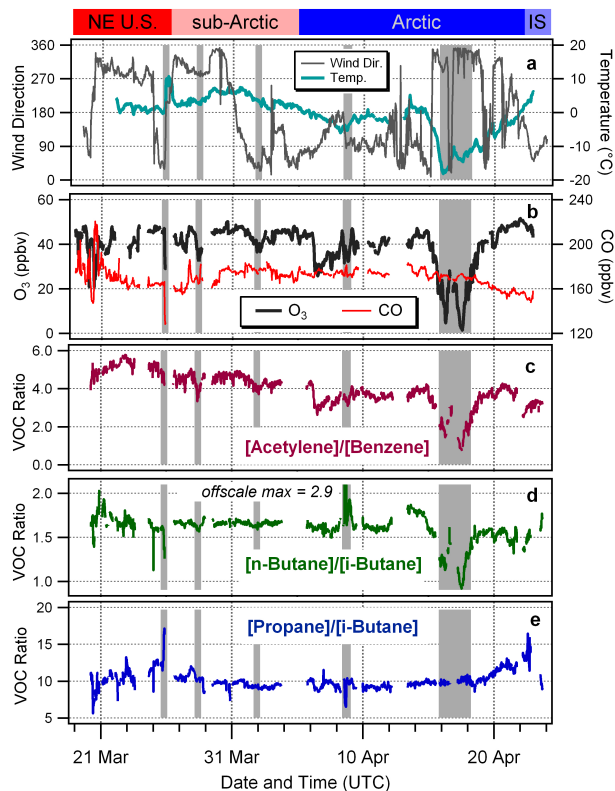


**Fig. 2.** Time series of (a) wind direction and ambient temperature, (b) O<sub>3</sub> and CO, (c) [Acetylene]/[Benzene] which is used as a marker for Cl and Br oxidation, (d) [n-butane]/[i-butane] which is used as a marker for Cl oxidation, (e) [Propane]/[i-butane] which is used as a marker for OH oxidation. The ICEALOT data subsets are delineated at the top. The grey bands highlight specific samples that are discussed in the text.

[Title Page](#)[Abstract](#)[Introduction](#)[Conclusions](#)[References](#)[Tables](#)[Figures](#)[◀](#)[▶](#)[◀](#)[▶](#)[Back](#)[Close](#)[Full Screen / Esc](#)[Printer-friendly Version](#)[Interactive Discussion](#)

Ozone variability and  
halogen oxidation

J. B. Gilman et al.

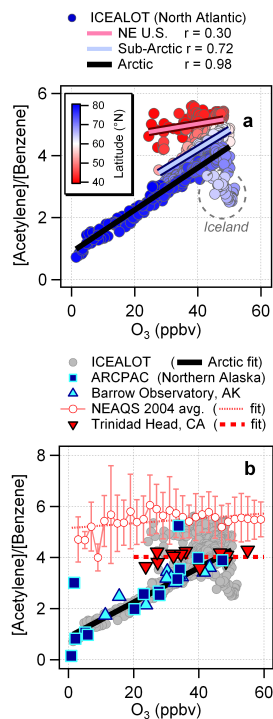


**Fig. 3. (a)** Scatter plots of  $[\text{Acetylene}]/[\text{Benzene}]$  versus  $\text{O}_3$  for the ICEALOT campaign. The data points have been colored by latitude. Linear fits and corresponding correlation coefficients for the NE US, sub-Arctic, and Arctic data subsets of the ICEALOT campaign are included. **(b)** Scatter plots of  $[\text{Acetylene}]/[\text{Benzene}]$  versus  $\text{O}_3$  for the flask samples from ARCPAC, Barrow, and Trinidad Head as well as the mean  $[\text{Acetylene}]/[\text{Benzene}] \pm 1 \sigma$  from NEAQS 2004. Linear fits to Trinidad Head and NEAQS 2004 datasets are shown. The ICEALOT data and fit to the Arctic data subset, which appear in panel (a), have been included in panel (b) for comparison.

Title Page

Abstract

Introduction

Conclusions

References

Tables

Figures

◀

▶

◀

▶

Back

Close

Full Screen / Esc

Printer-friendly Version

Interactive Discussion



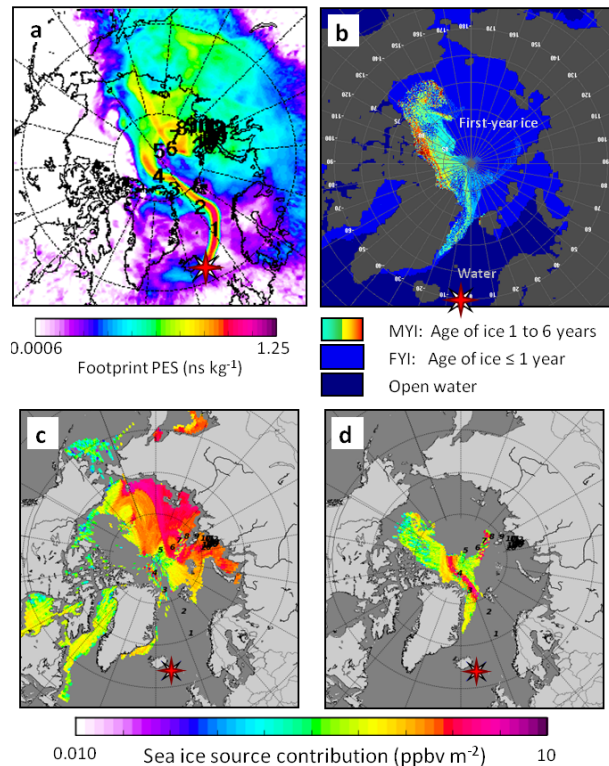


**Fig. 4.** (a) Circumpolar map of the FLEXPART modeled footprint potential emission sensitivity (PES) for the air mass sampled on 2 April 2008 at 00:00 UTC. The bold numbers represent the days of transport backward in time. (b) Map of the Arctic sea ice coverage colored by the modeled sea ice age for 1–7 April 2008. FLEXPART sea ice source contribution maps for (c) FYI and (d) MYI. The red star in panels (a-d) indicates the position of the R/V “Knorr” (62.9° N, 12.3° E).

Ozone variability and halogen oxidation

J. B. Gilman et al.

Title Page

Abstract Introduction

Conclusions References

Tables Figures

◀ ▶

◀ ▶

Back Close

Full Screen / Esc

Printer-friendly Version

Interactive Discussion



Ozone variability and  
halogen oxidation

J. B. Gilman et al.

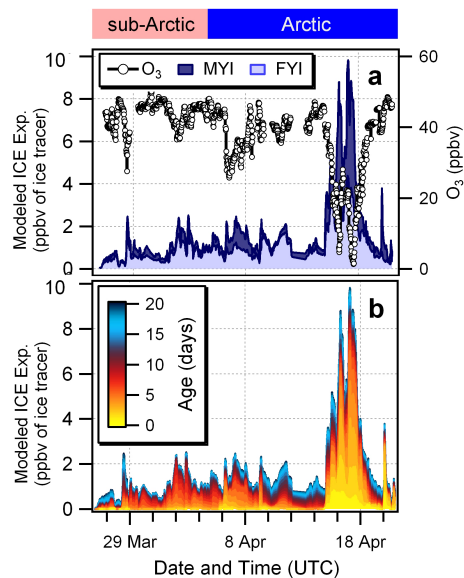


**Fig. 5.** (a) Time series of O<sub>3</sub> and the modeled FYI and MYI exposure for the sub-Arctic and Arctic data subsets from ICEALOT. MYI has been stacked on FYI so that the combined height represents the total ICE (FYI+MYI) exposure. (b) Time series of total ICE exposure colored by FLEXPART age.

Title Page

Abstract

Introduction

Conclusions

References

Tables

Figures

◀

▶

◀

▶

Back

Close

Full Screen / Esc

Printer-friendly Version

Interactive Discussion



Ozone variability and  
halogen oxidation

J. B. Gilman et al.

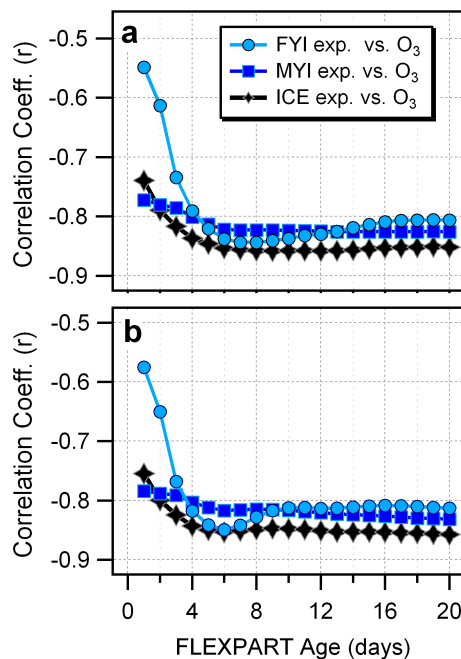


**Fig. 6.** Linear correlation coefficients for the modeled FYI, MYI, and ICE exposure versus O<sub>3</sub> as a function of the FLEXPART age for **(a)** the Arctic and **(b)** combined Arctic and sub-Arctic data subsets.

[Title Page](#)[Abstract](#)[Introduction](#)[Conclusions](#)[References](#)[Tables](#)[Figures](#)[I◀](#)[▶I](#)[◀](#)[▶](#)[Back](#)[Close](#)[Full Screen / Esc](#)[Printer-friendly Version](#)[Interactive Discussion](#)

## Ozone variability and halogen oxidation

J. B. Gilman et al.

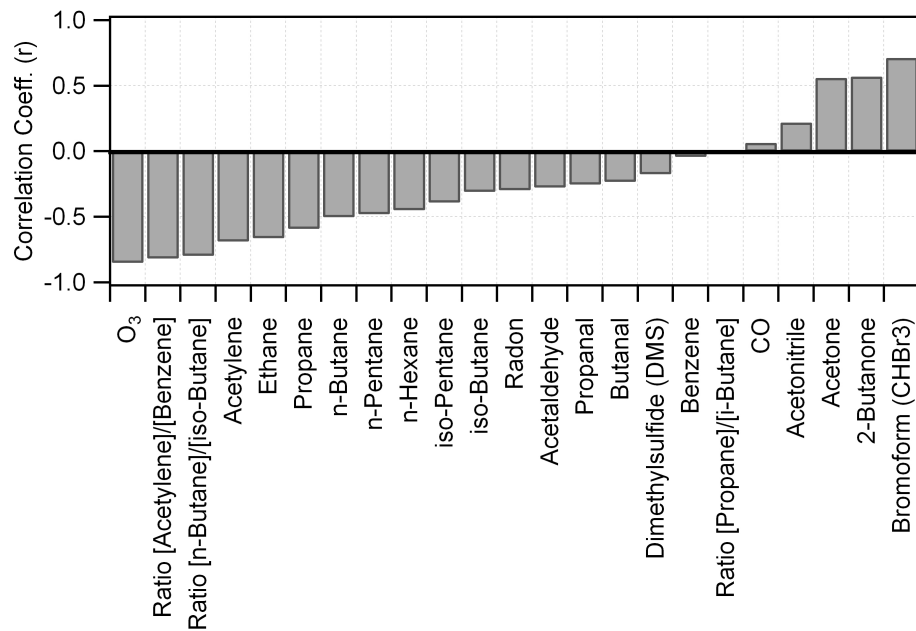


**Fig. 7.** Linear correlation coefficients for the 6-day cumulative modeled ICE exposure versus various gas-phase measurements made in the Arctic during ICEALOT.

Title Page

Abstract

Introduction

Conclusions

References

Tables

Figures

◀

▶

◀

▶

Back

Close

Full Screen / Esc

Printer-friendly Version

Interactive Discussion

